

Research on Effects of Chemical Erosion on Mechanical Properties of Q235 Steel Weld Seam

Liguo Yang^{a,b}, Anli Wu^{a,*}

^aSchool of Civil Engineering, Inner Mongolia University of Technology, Hohhot 010051, China

^bSchool of Science, Inner Mongolia University of Technology, Hohhot 010051, China
76351789@qq.com

Steel is mainly used in the chemical, mechanical, shipping and aerospace industries. The main connection method of steel is welding. Steel weld seams are weak areas in steel applications and vulnerable to the erosion of the chemical environment. In this paper, the corrosion behavior of steel welds and its mechanical properties are studied by taking Q235 steel as the base material and using arc welding, argon arc welding and acetylene-oxygen welding methods with chlorine corrosion solution concentration of 0.001 mol/L, 0.01 mol/L and 0.1 mol/L. The experimental results show that different welding methods, etching solution concentration, and erosion time can cause different corrosion behaviors and potential distributions. In the early stage of corrosion, the potential peaks are greatly different. As corrosion time passes by, the potential peaks become smoother. The mechanical properties of tensile strength, Brinell hardness and impact energy show a same pattern, and the weld strength decreases with the time of chlorine erosion.

1. Introduction

Q235 steel is easy to smelt, cheap, and exhibits excellent plasticity and welding ability, which can meet the requirements of ordinary parts and components in chemical and transportation industries (Zhang et al., 2017). Welding of Q235 steel is not limited by shape and easy to operate, which has good sealing performance, but welding defects in the welding process will make the structure a weak area of the entire component, and therefore the failure of the structure will occur first in the service process (Santa et al., 2011, Kim et al., 2015). Chemical erosion is a destructive phenomenon of steel in its environment and is a spontaneous process (Zhu et al., 2011). Corrosion can lead to a series material and energy contamination, causing huge economic losses and environmental pollution, which seriously leads accidents (Chen et al., 2013). Acid rain, dirt, etc. containing chemical substances can cause the aging of organic coatings and cause surface corrosion; the structures of steel in coastal areas can be eroded by Cl-salt mixed with sea breeze and increase the corrosion of steel welds (Erdem et al., 2016, Ghazanfari et al., 2012).

Currently, common steel structure welding methods include manual arc welding, tungsten arc welding, acetylene-oxygen welding, etc. (Guo et al., 2018). The welding process leads to a series of chemical reactions in the steel structure around the weld, including: heating and melting, solidification crystallization and solid phase transformation, etc., and the corrosion resistance at the weld joint is greatly reduced after a series of complex metallurgical processes (Dong et al., 2014, Zhang et al., 2015). Traditional weld seam corrosion detection methods use mechanical loss and mass loss as evaluation criteria, and electrochemical methods are measured by electrode potential method and electrochemical impedance spectroscopy (Evci et al., 2017). In chemically corrosive environments, steel weld seams act as weak points and the corrosion process causes damage to the mechanical properties of the steel weld (Aglan et al., 2013). In this paper, the Q235 steel weld seams were etched with chlorine salt, and the corrosion behavior was studied by scanning micro reference technology. The mechanical properties of chemically-eroded steel weld seams were also studied.

2. Study on corrosion behavior of welding seam of Q235 steel by scanning micro reference technology

Q235 steel has residual stress and welding defects in the welding process and becomes an area susceptible to corrosion. The chemical composition of the Q235 steel used in this article is shown in Table 1. Before the welding, the oil surface and oxide layer on the steel surface are removed; the welding joint is welded with "V" type argon arc welding; after the welding is completed, the welding port is polished with a polishing machine to be smooth, washed by ethanol for preparation. Corrosion samples were made of 0.01 mol/L NaCl solution. The steel welding samples were completely immersed in NaCl solution. The surface potential distributions in the three solutions were tested using the SMET module in the SMET/STM test system. The scanning range was $20\mu\text{m}\times 20\mu\text{m}$ and the test time is 5min, 15min, 30min and 60min. The samples of sodium chloride ethanol were both analytical reagents.

Figure 1 shows the variation of potential distribution in different weld zones of Q235 steel. It is obvious that the potential distributions of the four micro zones are different, which shows that there are different corrosion behaviors in the corrosion solution. The potential peak along the red line in Fig. 1(a) is bright, indicating that the area has already had an erosion failure point, resulting in dense electric field lines and sharp potential peaks. With the prolongation of erosion time, the erosion area continuously expanded and the potential peak of the test area decreased. When the erosion reached 60 min, the corrosion was relatively stable, the point corrosion became insignificant, and the peak potential did not change significantly.

Table1 Q235 steel chemical composition

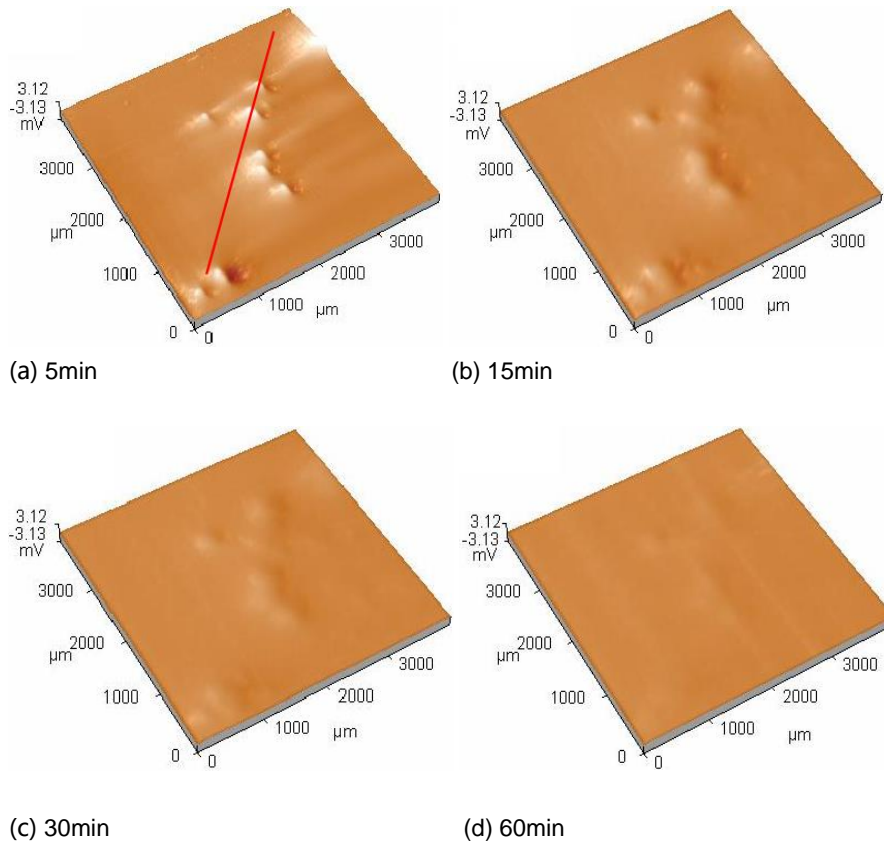


Figure 1: Variation of potential distribution in different weld zones of Q235 steel weld seams

3. Comparison of corrosion differences in different micro-zones of Q235 steel weld seams

3.1 Experiment

Corrosion of metal steel generally begins from a certain point of corrosion, pitting corrosion and local corrosion. Different welding shapes and different welding methods have different chemical corrosion conditions for steel welding samples. The Q235 steel from the previous section was selected from single weld butt welds, double weld butt welds and fillet welds, argon arc welding and acetylene - oxygen welding three

welding methods. With "V" cut welding, the weld sample is cut into 10mm*20mm blocks with the weld seam at the center of the weld sample, approximately 3mm-4mm. The potential synthesis probe uses Pt-Ir micro-scale and Ag/AgCl micro-scale, in which the Pt-Ir micro-scale is a scanning electrode. After the welding is completed, the welding port is polished with a polisher until it is smooth, and it is used after being cleaned with ethanol. Corrosion samples using 0.01mol/L NaCl solution, the steel welding samples completely immersed in NaCl solution, soak 60min.

3.2 Results and discussion

The weld seam of Q235 steel is sensitive to Cl, showing that the potential of the weld zone is significantly lower than that of the base metal zone, forming a larger potential difference.

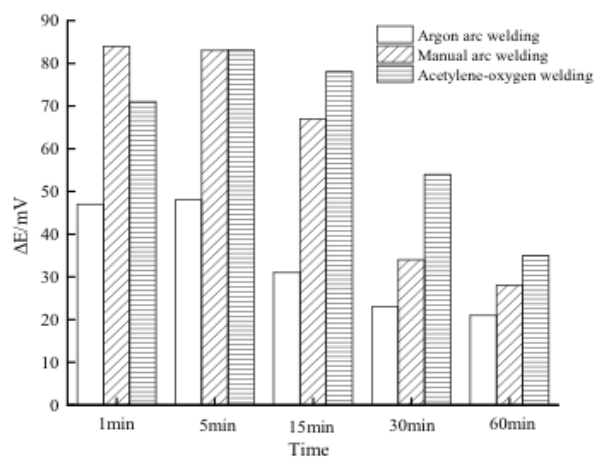


Figure 2: Comparison of different time potential differences of different welding methods for Q235 steel

Fig. 2 shows the comparison of different time potentials of different welding methods of Q235 steel. It can be clearly seen that the potential difference of the argon arc welding zone is the lowest, and the potential difference in different erosion time is 21-47mV; the potential difference of manual arc welding is the highest, up to 84mV, 15min before erosion. But when the erosion time is beyond 15min, the acetylene-oxygen welding potential difference is greater than the argon arc welding and manual arc welding. It can be inferred that the seriousness of galvanic corrosion is: acetylene-oxygen gas welding > manual arc welding > argon arc welding.

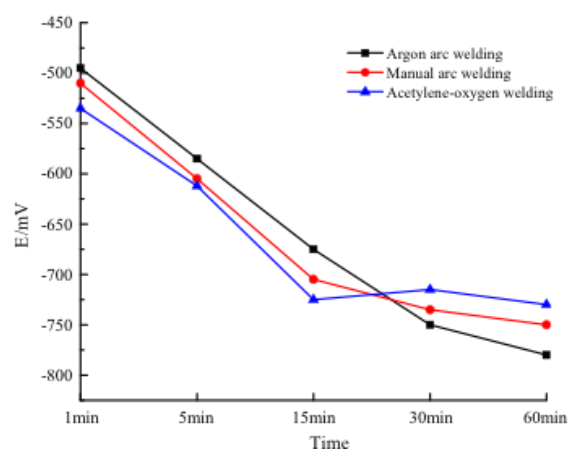


Figure 3: Comparison of average potential of weld samples of different Q235 steels at different time

Fig. 3 compares the average potentials of different welding methods of Q235 steel at different times. It can be seen that the magnitude of the potential in 15 minutes is: argon arc welding > manual arc welding > acetylene-oxygen welding, and the when the erosion time is beyond 15 minutes, the potential growth rate of argon arc welding is the lowest, followed by manual arc welding and acetylene-oxygen welding, in which the potential of

argon arc welding slightly rises at 30 minutes of erosion; when the erosion time is greater than 30 minutes, the potential size is: acetylene-oxygen welding> manual arc welding> Argon arc welding.

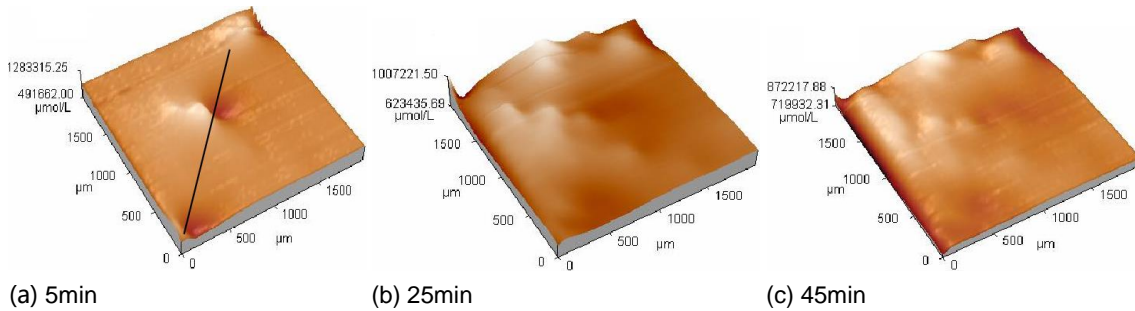


Figure 4: Chloride ion distribution of Q235 steel welds at different time

Fig. 4 shows the chloride ion distribution of Q235 steel weld seams at different times. The more severe the chlorine erosion is, the higher the peak value of chloride ion concentration is, and the three larger chloride peaks appear at the initial stage of corrosion; at 25 minutes, there are more and more different sizes of chloride peaks, indicating that the pitting area starts to aggregate; the chloride peak distribution is even at 45 min. Fig. 5 shows the distribution of corrosion potentials of Q235 steel welds at different times. The performance is similar to that of chloride ions. Three large corrosion potential peaks appear at the beginning of corrosion, and the surface of the sample shows uneven pitting corrosion at 30 minutes, and a large number of potential peaks appeared on the surface; the potential peaks became flattened after 50 minutes of erosion.

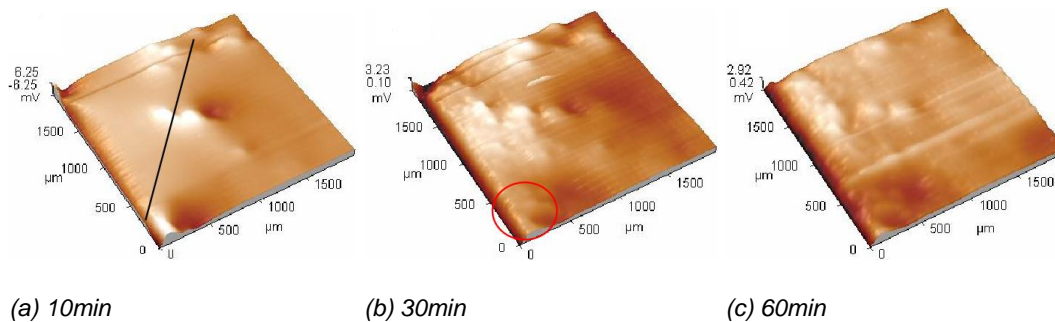


Figure 5: Corrosion potential distribution of Q235 steel weld seams at different time

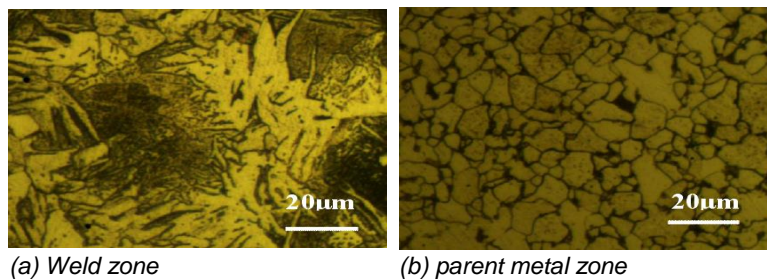


Figure 6: The microstructure of weld zone and parent metal zone of Q235 welding sample

4. Study on mechanical properties of weld seams in chemically erosion steel

4.1 Experiments

The treatment process of Q235 steel is consistent with that in section 3. The welding method for steel weld seam is submerged arc welding. The samples are immersed in 0.01 mol/L NaCl solution from January to October. The Brinell hardness, the impact resistance and tensile strength of each sample are tested respectively. The impact test specimens were selected as "V" type notched welding specimens, and the

specific test method was referred to the *Impact Test Method For Welded Joints*. The impact test was conducted on an impact tester. The Brinell hardness test was performed on a Brinell hardness tester of HB-3000C, and the indenter diameter is 5mm. The tensile strength test was conducted in accordance with the specification *Tensile Test Method for Welded Joints*.

4.2 Experimental results

Tensile properties, fatigue properties and impact properties are important indicators for measuring the mechanical properties of steel. Figure 7 shows the weld hardness of Q235 steel at different erosion time. It can be clearly seen that the hardness of Q235 steel decreases with the increase of erosion time. The hardness of the weld layer near the inner wall, the hardness of the middle weld layer and the hardness of the outer wall of the weld layer show the same pattern. Fig. 8 shows the impact energy of Q235 steel welds at different erosion times. The overall performance is that as the erosion time increases, the impact energy decreases, and the impact energy at the 3d of chemical erosion appears a slight increase. This may be caused by experimental errors. Figure 9 shows the tensile strength of Q235 steel weld seams at different erosion times. The law of tensile strength shows the same rules as Brinell hardness and impact energy. In summary, as a weak zone in steel applications, steel weld seams are prone to chemical attack, and after the chemical erosion, the intensity index decreases greatly.

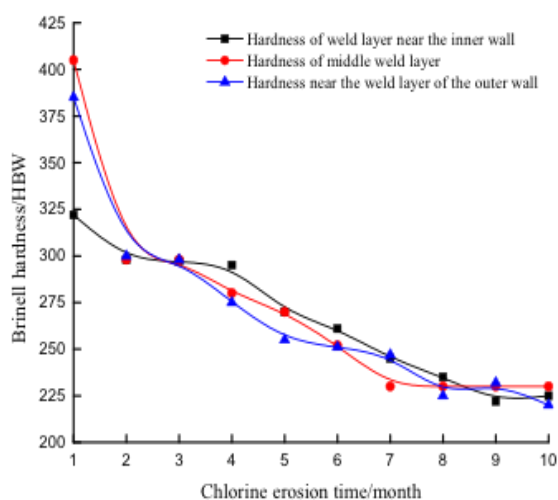


Figure 7: Hardness of Q235 steel weld seams at different erosion times

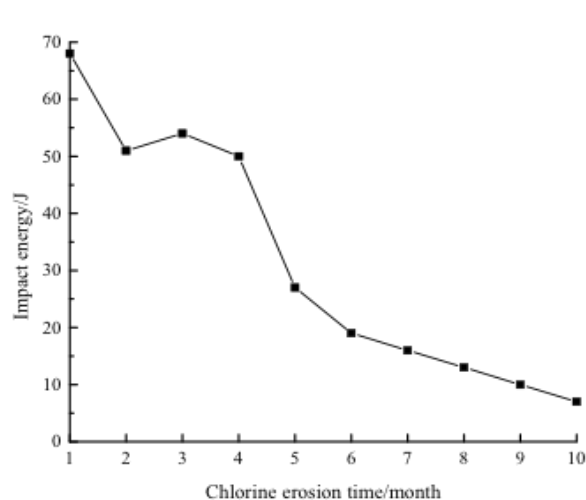


Figure 8: Impact energy of Q235 steel weld seams at different erosion times

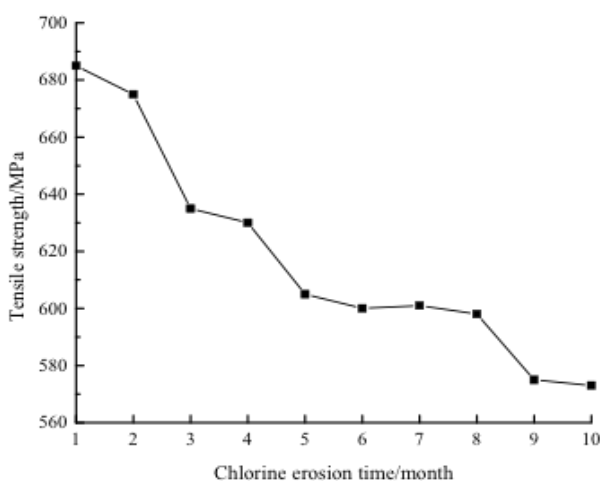


Figure 9: Tensile strength of Q235 steel weld seams at different erosion times

5. Conclusion

In this paper, the corrosion of Q235 steel welded by chlorine salt was tested. The corrosion behavior was studied by scanning micro-reference technology, and the mechanical properties of chemically-eroded steel weld steams were studied. The specific experimental results are as follows:

- (1) With the prolongation of erosion time, the erosion area continuously expands and the peak value of the potential in the test area decreases. When the erosion reaches 60 min, the corrosion is relatively stable, the point corrosion becomes insignificant, and the peak potential does not change significantly.
- (2) The corrosion potential profile of Q235 steel weld steams at different times is approximately the same as that of chloride ions. Three large corrosion potential peaks appear at the beginning of corrosion, and the surface of the sample shows uneven pitting corrosion at 30 minutes and appears a large number of potential peaks; the potential peaks become flattened when eroded to 50 min.
- (3) Tensile strength, Brinell hardness, and impact energy show the same pattern. With the extension of the chlorine erosion time, the strength of the weld seam decreases. As a weak area in the steel application, the strength index after chemical erosion decreases greatly.

References

- Aglan H.A., Ahmed S., Prayakarao K.R., and Fateh M., 2013, Effect of preheating temperature on the mechanical and fracture properties of welded pearlitic rail steels, *Engineering*, 5(11), 837-843, DOI: 10.4236/eng.2013.511101.
- Chen X.Z., Huang Y.M., Shen Z., Chen J., Lei Y.C., and Zhou J.Z., 2013, Effect of thermal cycle on microstructure and mechanical properties of CLM steel weld CGHAZ, *Science & Technology of Welding & Joining*, 18(4), 272-278, DOI: 10.1179/1362171812Y.0000000095
- Dong H., Hao X., and Deng D., 2014, Effect of welding heat input on microstructure and mechanical properties of hsla steel joint, *Metallography Microstructure & Analysis*, 3(2), 138-146, DOI: 10.1007/s13632-014-0130-z.
- Erdem M., Altuğ M., and Karabulut M., 2016, Investigation of mechanical, microstructural, and machining properties of aisi 420 martensitic stainless steel welded by laser welding, *International Journal of Advanced Manufacturing Technology*, 85(1-4), 481-492.
- Evcı C., H Isik, adn Macar M., 2017, Effect of welding wire and groove angle on mechanical properties of high strength steel welded joints, *Materialwissenschaft Und Werkstofftechnik*, 48(9), 912-921, DOI: 10.1002/mawe.201700033.
- Ghazanfari H., Naderi M., Iranmanesh M., Seydi M., and Poshteban A., 2012, A comparative study of the microstructure and mechanical properties of htla steel welds obtained by the tungsten arc welding and resistance spot welding, *Materials Science & Engineering A*, 534(2), 90-100, DOI: 10.1016/j.msea.2011.11.046.
- Guo W., Wan Z., Peng P., Jia Q., Zou G., and Peng Y., 2018, Microstructure and mechanical properties of fiber laser welded QP980 steel, *Journal of Materials Processing Technology*, 256, DOI: 10.1016/j.jmatprotec.2018.02.015.
- Kim H.J., Jeon S.H., Kim S.T., and Park Y.S., 2015, Influence of the shielding gas composition on the passive film and erosion corrosion of tube-to-tube sheet welds of hyper duplex stainless steel, *Corrosion Science*, 91, 140-150, DOI: 10.1016/j.corsci.2014.11.014.
- Santa J.F., Blanco J.A., Giraldo J.E., 2011, Cavitation erosion of martensitic and austenitic stainless steel welded coatings, *Wear*, 271(9), 1445-1453, DOI: 10.1016/j.wear.2010.12.081
- Zhang S., Wang S., Wu C.L., Zhang C.H., Guan M., and Tan, J.Z., 2017, Cavitation erosion and erosion-corrosion resistance of austenitic stainless steel by plasma transferred arc welding, *Engineering Failure Analysis*, 76, 115-124, DOI: 10.1016/j.engfailanal.2017.02.007.
- Zhang W., Zhong Z., and Kang S., 2015, Microstructures and mechanical properties of a martensitic steel welded with flux-cored wires, *International Journal of Coal Science & Technology*, 3(3), 254-260, DOI: 10.1007/s40789-015-0082-1.
- Zhu Q., Lei Y.C., Chen X.Z., Ren W.J., Ju X., and Ye Y.M., 2011, Microstructure and mechanical properties in tig welding of clam steel, *Fusion Engineering and Design*, 86(4), 407-411, DOI: 10.1016/j.fusengdes.2011.03.070.